Journal of Organometallic Chemistry, 403 (1991) 195–208
Elsevier Sequoia S.A., Lausanne
JOM 21315

Dynamic NMR studies of ring rotation in substituted ferrocenes and ruthenocenes

Edward W. Abel, Nicholas J. Long, Keith G. Orrell *, Anthony G. Osborne and Vladimir Šik

Department of Chemistry, The University, Exeter EX4 4QD (UK)

(Received July 30th, 1990)

Abstract

Variable temperature ^{1}H and $^{13}C\{^{1}H\}$ NMR studies on 1,1′,3,3′-tetra(alkyl)-ferrocenes and -ruthenocenes (alkyl = t-pentyl,t-butyl) have provided accurate barrier energies for restricted rotations of the substituted cyclopentadienyl rings. Energies ($\Delta G^{\ddagger}$ (298.15 K)) are in the range 40–57 kJ mol^{-1} and are dependent on the 'sandwich' metal (Fe ≫ Ru) and alkyl substituent (t-pentyl > t-butyl). Ring rotation in 1,1′,3,3′-tetra(phenyl)ferrocene was too rapid for measurement even at 173 K. Spectral changes were analysed primarily on the basis of exchange between a mirror pair of structures having both 5-membered rings eclipsed and the alkyl substituents staggered. In the case of 1,1′,3,3′-tetra(t-butyl)ferrocene a pair of staggered ring rotamers also contributed to the observed NMR bandshape changes.

Introduction

Energy barriers to ring rotation in unsubstituted cyclopentadienyl (Cp) metal sandwich complexes are generally low. For those few compounds which have been studied, activation energies have been determined from both solid state and solution NMR measurements of spin-lattice relaxation times [1]. In lightly substituted ferrocenes, e.g. $[(\eta^5\text{-}C_5H_5)Fe(\eta^5\text{-}C_5H_4R)]$ (R = n-Bu,t-pentyl [2], or CHO [3]) and related sandwich complexes e.g. $[(\eta^5\text{-}C_5H_5)M(\eta^4\text{-cod})]$ (M = Rh, Ir; cod = cycloocta-1,5-diene) [4] C_5H_5 ring rotation rates are again only measurable from NMR T_1 data. When the Cp rings carry numerous bulky substituents the barriers to rotation increase as expected and rotation rates are reduced sufficiently to lie within the timescale of NMR chemical shift modulation.

Approximate energies of rotation deduced from NMR band coalescence measurements have been obtained for a variety of substituted metallocenes. These include 1,1′,3,3′-tetra(trimethylsilyl)ferrocene and -titanocene dichloride [5,6], 1,1′,3,3′-tetra(t-butyl)ferrocene [7] and other more heavily substituted ferrocenes [8–10].

We have now applied the more rigorous approach of total NMR bandshape analysis, to the $^{1}H/^{13}C$ spectra of 1,1′,3,3′-tetra(t-butyl)ferrocene, 1,1′,3,3′-tetra(t-pentyl)ferrocene, along with the corresponding ruthenocene complexes. As far as we

0022-328X/91/$03.50

are aware these are the first reported values of ring rotation energies for substituted ruthenocenes.

We have also investigated the solution dynamics of 1,1′,3,3′-tetra(phenyl)ferrocene in the light of previous inconclusive studies on 1,1′,2,2′,3,3′,4,4′-octa(phenyl) ferrocene [11]. We also report variable temperature CP-MAS NMR spectra of the solid 1,1′,3,3′-tetra(t-pentyl)ferrocene.

Experimental

General

All preparations were carried out using standard Schlenk techniques [12]. All reactions were performed under purified nitrogen using freshly distilled, dried and degassed solvents.

Infrared spectra were recorded on a Perkin Elmer 881 infrared spectrophotometer, calibrated from the 1602 cm^{-1} signal of polystyrene.

Elemental analyses were performed by Butterworth Laboratories Ltd., Teddington, Middlesex, London and by C.H.N. Analysis, South Wigston, Leicester.

^{1}H and $^{13}C\{^{1}H\}$ NMR spectra were recorded on a Bruker AM250 FT spectrometer, operating at 250.13 and 62.90 MHz respectively. The spectra were recorded on CD_2Cl_2 or $CDCl_3$ solutions with chemical shifts being quoted relative to Me_4Si as internal standard.

A standard B-VT1000 variable temperature unit was used to control the probe temperature, with the calibration of this unit being checked periodically against a Comark digital thermometer. The temperatures are considered accurate to $\pm 1°C$. Bandshape analyses were performed using modified versions of the program DNMR of Kleier and Binsch [13,14].

$^{13}C\{^{1}H\}$ NMR CP-MAS solid state spectra were recorded on a Varian VXR 300 spectrometer operating at 75.43 MHz for carbon-13. Typical operating conditions were, acquisition time 13-30 ms, relaxation delay 1–5 s, contact time 3 ms. Normal CP-MAS spectra were recorded in the temperature range ambient (22°C) to −120°C. A non-quaternary suppression (NQS) spectrum [15] at ambient temperature was also recorded to aid spectral assignment.

Synthesis of substituted ferrocenes and ruthenocenes

1,1′,3,3′-Tetra(t-butyl)ferrocene (1) and 1,1′,3,3′-tetra(t-pentyl)ferrocene (2). These species were prepared using a similar method to that described by Leigh [16]. The only modifications were the time and temperature of reaction, where t-butyl and t-pentyl substitutions took 4 and 5 h respectively and were carried out at 60 and 40°C respectively. These previously known species were characterised by spectroscopic studies and melting temperatures of 192–194°C and 111°C for **1** and **2** respectively (lit. values [16], m.p. 194–196 and 110°C respectively).

1,1′,3,3′-Tetra(t-butyl)ruthenocene (3) and 1,1′,3,3′-tetra(t-pentyl)ruthenocene (4). These compounds were also prepared in an analogous fashion to that described by Leigh [16]. **3** was isolated as an off-white powder after a reaction of 48 h at 60°C in a yield of 47%, m.p. = 190–192°C. Anal. Found: C, 68.9; H, 9.4. $C_{26}H_{42}Ru$ calcd.: C, 68.6; H, 9.2%. **4** was also an off-white powder formed from a reaction lasting 48 h at 40°C. Yield, 35%, m.p. = 104–106°C. Anal. Found: C, 69.4; H, 10.0. $C_{30}H_{50}Ru$ calcd.: C, 70.5; H, 9.8%.

1,1',3,3'-Tetra(phenyl)ferrocene (5). This compound was synthesized via a number of steps:

(a) Synthesis of 1,3-diphenylcyclopentadiene (I). This was prepared following the method described by Drake and Adams [17].

(b) Synthesis of lithium 1,3-diphenylcyclopentadienide (II). To a stirred solution of I (1.0 g, 4.6 mol) in benzene (60 cm^3) was added 1.45 *M* n-butyllithium in hexane (3.24 cm^3, 4.7 mmol). Immediately on addition, a thick white precipitate was formed which was then stirred for approximately one hour. The mixture was then evaporated to dryness to leave an air-sensitive, off-white powder (II). Yield, 0.81 g (79%).

(c) Synthesis of 1,1',3,3'-tetra(phenyl)ferrocene. A solid mixture of anhydrous $FeCl_2$ (0.19 g, 1.5 mmol) [18] and II (0.79 g, 3.13 mmol) was combined with tetrahydrofuran (25 cm^3). The brown mixture was stirred overnight. The solvent was removed and the resulting solid was added to toluene (100 cm^3) and heated to boiling in air. The hot solution was filtered rapidly and reheated to boiling. The mixture was then evaporated to dryness and the crude orange-red solid subjected to column chromatography on neutral grade II alumina. Using hexane as eluent, two fractions were collected. The colourless first fraction was 1,3-diphenylcyclopentadiene, whilst the orange-red second fraction contained the product. After cooling the solution to $-20\,^\circ C$ overnight, red crystals were obtained in a yield of 0.38 g (52%). This known compound was characterised by spectroscopic studies and a melting temperature of 222–223 °C (lit. value [19], m.p. 220–222 °C).

Results and discussion

The ambient temperature ^1H and ^{13}C NMR spectra of the complexes **1–4** clearly indicated rapid rotation of the 5-membered cyclopentadienyl rings since signals corresponding to a single R substituent environment and two ring C–H environments were detected (Tables 1 and 2). On cooling the solutions of the complexes to $-40\,^\circ C$ or below, changes occurred in both the ^1H and ^{13}C spectra consistent with a

Table 1

^1H NMR parameters for 1,1',3,3'-tetrasubstituted ferrocenes in CD_2Cl_2 solution at ambient and low temperatures

Substituent	Temperature (°C)	δ (ring)	δ (alkyl or aryl group)
t-butyl	+30	3.96(d)[1.6] [a]	1.24(s)
		3.87(t)[1.4] [a]	
	−80	3.91 [b]	1.13 [b]
		3.88 [b]	1.11 [b]
		3.80 [b]	
t-pentyl	+30	3.95(d)[1.5] [a]	1.30–1.20(m) [c]
		3.87(t)[1.6] [a]	0.58(t)[7.5] [a,d]
	−40	3.88 [b]	1.30–1.15(m) [c]
		3.84 [b]	0.55(t)[7.5] [a,d]
		3.78 [b]	0.45(t)[7.5] [a,d]
phenyl	+30	4.67(t)[1.5] [a]	7.21(m)
		4.48(d)[1.5] [a]	
	−100	4.67 [b]	7.20 [b]
		4.43 [b]	

[a] *J*(HH). [b] Broadened signals. [c] Many overlapping signals. [d] Due to CH_3CH_2 of t-pentyl group.

Table 2

$^{13}C\{^1H\}$ NMR data for 1,1′,3,3′-tetrasubstituted metallocenes in CD_2Cl_2 solution at ambient and low temperatures

Metal	Substituent	Temperature (°C)	δ (quaternary ring carbons)	δ (ring C–H carbons)	δ (alkyl group carbons)
Fe	t-butyl	+30	100.30	64.10	32.35 [a]
				63.70	31.20 [b]
		−60	101.72	65.24	32.64 [a]
			98.20	64.21	31.79 [a]
				63.67	31.44 [b]
					30.91 [b]
Ru	t-butyl	+30	105.36	68.00 [c]	32.28 [a]
					30.76 [b]
		−80	106.59	69.09	32.62 [a]
			103.09	68.57	31.87 [a]
				67.28	31.03 [b]
					30.79 [b]
Ru	t-pentyl	+30	103.96	69.69	38.36
					33.77
				68.40	29.89
					27.42
					9.50 [d]
					38.90
					38.19
					34.02
		−70	104.64	70.68	33.75
			101.15	69.03	32.56?
				67.66	30.00?
					27.00
					25.66
					10.01 [c,d]

[a] CH_3 of t-butyl group. [b] Quaternary C of t-butyl group. [c] Two signals overlapping. [d] Due to CH_3CH_2 of t-pentyl group.

deceleration of the ring rotation rate and an eventual 'freezing' into a single rotameric form. In the ^1H spectra the two ring-proton signals broadened and split into three at the lowest temperatures whereas all substituent signals split into pairs. In the ^{13}C spectra the two ring methine carbon signals split into three whereas the single quaternary ring carbon signal and all substituent carbon signals split into pairs. The resulting low temperature spectra are consistent only with a single type of rotameric structure.

A full analysis of the rotational problem shows there to be five rotamers with eclipsed Cp rings (labelled *e*) and five with fully staggered rings (labelled *s*) (Fig. 1). Following the approach of Okuda and Herdtweck for 1,1′,3,3′-tetra(trimethylsilyl) ferrocene [6] the relative ground state energies of these species are assumed to be due solely to the interannular repulsions of the alkyl substituents. These are treated additively, a notional value of 0.5 being attributed to the mutual interaction of two fully staggered groups in different rings and a value of 1 for interaction of two eclipsed R groups. These total values are then attached to the *e* or *s* labels as subscripts and assigned to the ten rotameric species. The enantiomeric pairs of C_2

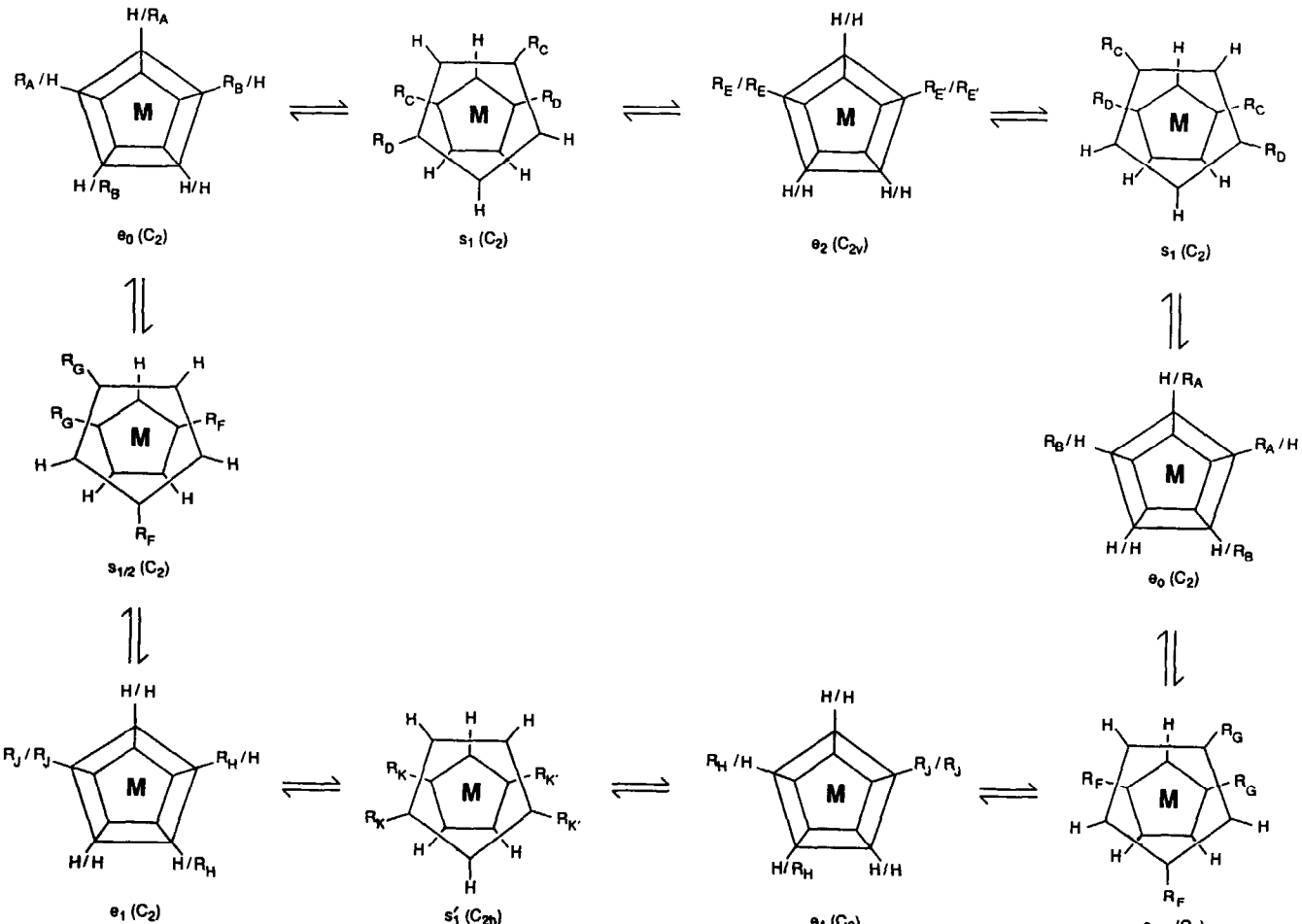

Fig. 1. The ten eclipsed (e) and fully staggered (s) forms of 1,1′,3,3′-tetrasubstituted metallocenes showing the interconversion pathway resulting from Cp ring rotations. The structures are labelled according to ref. [6].

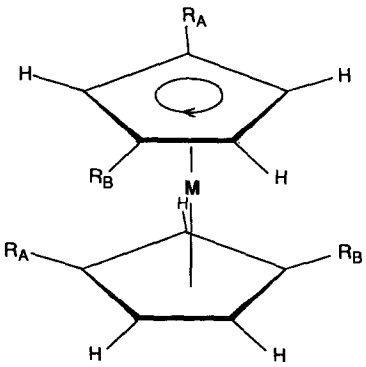

Fig. 2. The lowest energy rotameric form of 1,1′,3,3′-tetrasubstituted metallocenes. This structure corresponds to the $e_0(C_2)$ structure in the top left corner of Fig. 1.

symmetry are accordingly labelled e_0, e_1, $s_{1/2}$ and s_1, and the singular structures, possessing C_{2v} and C_{2h} symmetries are labelled e_2 and s_1' respectively. All these structures are interconverted by relative rotation of the two Cp rings by the pathway depicted in Fig. 1. The ground-state structure e_0 (and its enantiomer) thus correspond to the eclipsed ring structures with the four R substituents in a fully staggered arrangement, and eclipsed only by ring protons. This structure is represented more conventionally by Fig. 2 and corresponds to the structure in the top left corner of Fig. 1. The other structures in Fig. 1 are reached by clockwise or anti-clockwise rotation of the *upper* Cp ring with the lower ring held fixed. The e_0 structures of C_2 symmetry closely correspond to the X-ray crystal structure of 1,1′,3,3′-tetra(trimethylsilyl)ferrocene [6], and are similar to that of 1,1′,3,3′-tetra(t-butyl)ferrocene [20] which lies between the e_0 and $s_{1/2}$ structures, but somewhat closer to the eclipsed form. Such agreement lends credence to this rather simplistic method of assessing relative energies of rotamers. The low temperature solution $^1H/^{13}C$ NMR spectra of the complexes **1–4** are fully consistent with the e_0 rotamers being the ground state pair. However, this structural type cannot be distinguished by NMR from the other structures of C_2 symmetry, namely e_1, $s_{1/2}$ and s_1, as can be seen by reference to Table 3 which lists the numbers of ^1H and ^{13}C NMR signals expected for each rotamer type. Nevertheless, it would appear to be a very reasonable assumption that

Table 3

Numbers of $^1H/^{13}C$ NMR signals expected for rotamers of 1,1′,3,3′-tetra(alkyl)metallocenes

Group	Nucleus	Expt.[a]	e_0	e_1	e_2	$s_{1/2}$	s_1	s_1'
Ring C-H	^1H	3	3	3	2	3	3	2
	^{13}C	3	3	3	2	3	3	2
Ring$\gtrless$C–	^{13}C	2	2	2	1	2	2	1
t-Butyl	^1H	2	2	2	1	2	2	1
	^{13}C	4	4	4	2	4	4	2
t-Pentyl	^1H	6?	6	6	3	6	6	3
	^{13}C	8?	8	8	4	8	8	4

[a] Limiting low temperature spectra.

the observed NMR bandshape changes are due to restricted rotation of the Cp rings producing exchange between the enantiomeric e_0 pair of rotamers. This e_0–e_0 exchange may be envisaged as occurring via the $s_{1/2}$, e_1 and s_1' structures and/or via the s_1 and e_2 structures (Fig. 1). Complete rotation of the Cp rings will involve all intermediate structures. However, the highest energy e_2 structure may prevent complete 360° rotations from occurring, in which event the rings will oscillate between all the other structures. Whilst complete Cp ring rotations would appear to be intuitively more reasonable, it should be pointed out that, because of the absence of any contribution of the e_2 rotamer to the observed NMR bandshapes, NMR cannot distinguish between Cp ring rotations and oscillations. However, the energy barriers measured must be interpreted as ΔE ($e_1/s_1' - e_0$), rather than ΔE ($e_2 - e_0$) since the spectra will be sensitive only to the rates for the lower energy pathway. It should be noted that this conclusion is contrary to that reached by Okuda and Herdtweck for 1,1′,3,3′-tetra(trimethylsilyl)ferrocene [6].

Carbon-13 bandshape analyses

For 1,1′,3,3′-tetra(t-butyl)ferrocene (**1**) and 1,1′,3,3′-tetra(t-butyl)ruthenocene (**3**) the signals of the metal and quaternary carbons of the substituents were used for the bandshape analyses as they exhibited the largest exchange effects. The spectra of the ferrocene complex (**1**) are shown in Fig. 3. The static spectrum at −60 °C clearly displays both pairs of methyl and quaternary carbon signals with the latter pair significantly sharper, presumably due to the longer spin–spin relaxation time of the quaternary carbons. These different natural line widths were accounted for in the subsequent bandshape analyses by attributing different T_2^* values to the signals.

The total dynamic problem expressed in terms of the substituent R spins (^{13}C or ^1H) is:

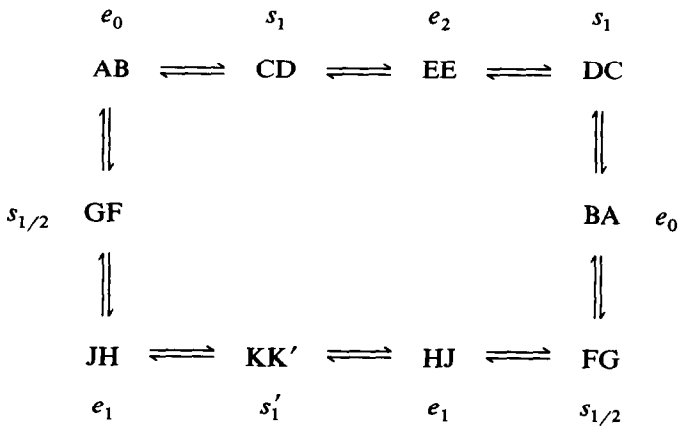

The labelling of nuclei refers to Fig. 1. Since only the e_0 pair of rotamers is being considered, however, the problem simplifies to AB ⇌ BA which reduces further to A ⇌ B in the absence of any scalar coupling between the R substituents. Thus, the bandshape analysis problem consists of direct exchanges between two equally populated methyl and quaternary carbon sites. Good agreement was obtained between experimental and computer synthesised spectra of **1** in the temperature range −60 to 15 °C (Fig. 3) from which reliable activation energy data were obtained (see later). The same procedure was adopted for the ruthenocene complex

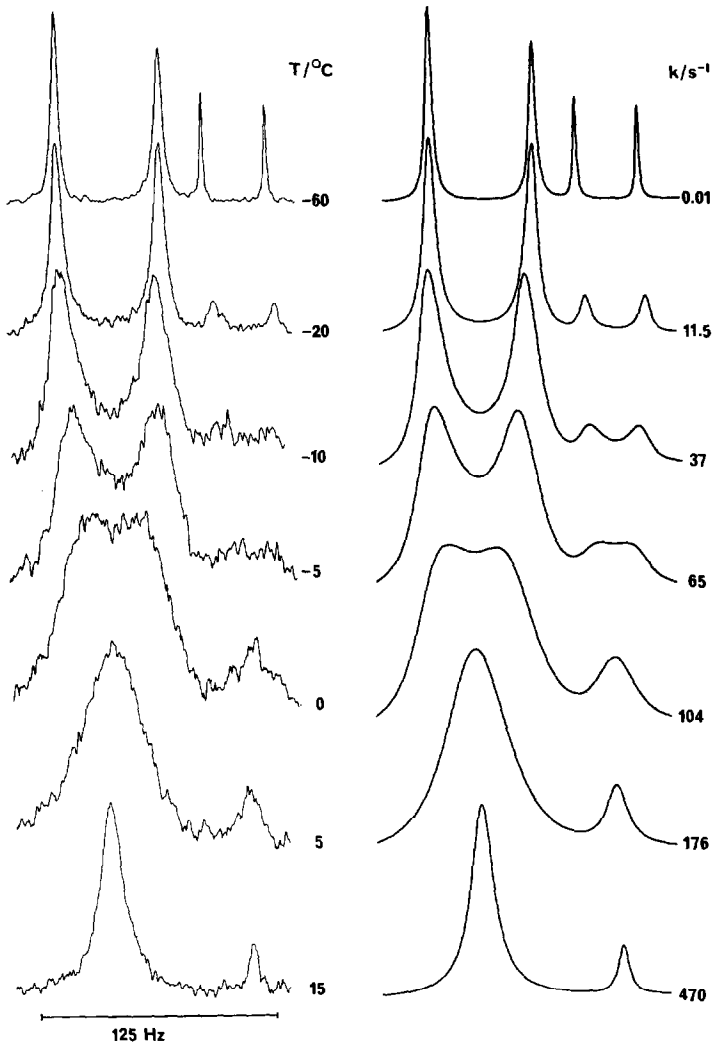

Fig. 3. Carbon-13 NMR spectra (t-butyl region) of 1,1′,3,3′-tetra(t-butyl)ferrocene in the temperature range −60 °C to ambient. Computer synthesised spectra with best-fit rate constants are shown alongside.

3, in this case the temperature range over which fittings were performed being −80 to −40 °C.

The ^{13}C spectra of 1,1′,3,3′-tetra(t-pentyl)ruthenocene (**4**) were rather complex in the t-pentyl region and bandshape analysis was applied to the less crowded quaternary ring carbon signals. Spectral simulations in this case were confined to the temperature range −70 to −10 °C.

Hydrogen-1 bandshape analyses

Variable temperature ^{1}H spectra of 1,1′,3,3′-tetra(t-pentyl)ferrocene (**2**) showed substantial changes due to the varying rates of rotation of the Cp rings, and thus they were chosen as the vehicle for the dynamic bandshape analysis. The methyl signals of the ethyl portion of the t-pentyl group (i.e.: $C(CH_3)_2CH_2CH_3$) were

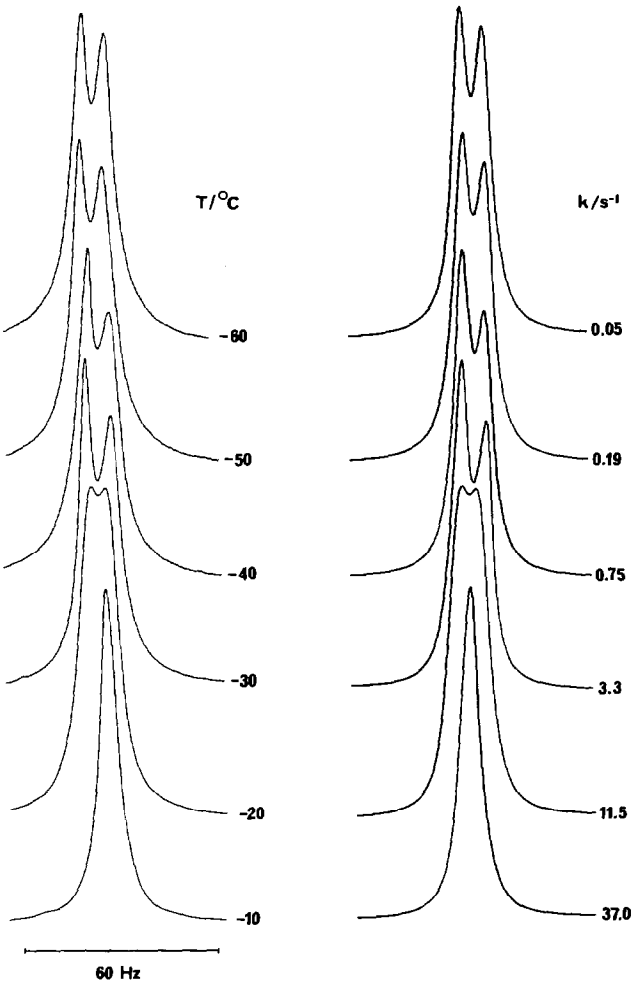

Fig. 4. Hydrogen-1 NMR spectra (t-butyl region) of 1,1′,3,3′-tetra(t-butyl)ferrocene showing the asymmetric decoalescence of the t-butyl signal on cooling. Computer fitted spectra shown alongside are based on case b of Fig. 5.

chosen for the fittings. These changed from a single 1 : 2 : 1 triplet at ambient temperature to two 1 : 2 : 1 triplets at −40 °C. Computer synthesised spectra based on $AX_2 \rightleftharpoons BX_2$ exchange were fitted to the experimental spectra in the temperature range −40 to 20 °C and the resulting rate constant/temperature data converted to activation energies via the Arrhenius and Eyring equations.

Variable temperature ^1H spectra, in addition to ^{13}C spectra, were also recorded for 1,1′,3,3′-tetra(t-butyl)ferrocene (**1**). The single t-butyl signal at ambient temperature broadened on cooling and eventually split into two signals when the Cp ring rotation became sufficiently slow. However, this decoalescence effect does not occur in a symmetrical manner as can be seen from the experimental spectra in Fig. 4. This asymmetry arising from the somewhat broader nature of the low frequency member of the doublet was apparent in the previous studies on this compound [7] and on the trimethylsilyl analogue [6] but was not commented on in either case. We

are convinced that it is a real spectral effect and not some instrumental artefact and have explored it further by means of a very accurate set of expanded spectra in this region.

The most reasonable explanation of this effect stems from the previous assumption that only the e_0 pair of rotamers contributes to the NMR bandshapes. This does appear to be fully valid for all the ^{13}C spectra of the complexes and for the ^1H spectra of **2**, but not for the ^1H spectrum of **1**. Reference back to Fig. 1 shows that the second lowest energy pair of rotamers is likely to be the $s_{1/2}$ pair and so it is quite possible that there may be a small contribution to the observed NMR bandshape by these species. Each would produce a pair of t-butyl signals, labelled F & G in Fig. 1. The dynamic R spin problem would therefore become:

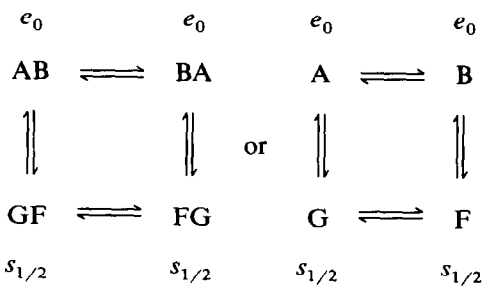

Under conditions of fast exchange, a single averaged t-butyl signal would occur, as observed, whereas in the slow exchange limit four signals would be expected. In fact, only two were observed, suggesting either that the population of the $s_{1/2}$ rotamers had become negligibly small at the lowest temperatures or that their t-butyl chemical shifts had become indistinguishable from those of the e_0 pair. After carefully testing both possibilities we concluded that the latter explanation was more likely. The temperature at which the $s_{1/2}$ pair contributed most to the observed bandshape was $-30\,°C$, and the asymmetric doublet absorption at this

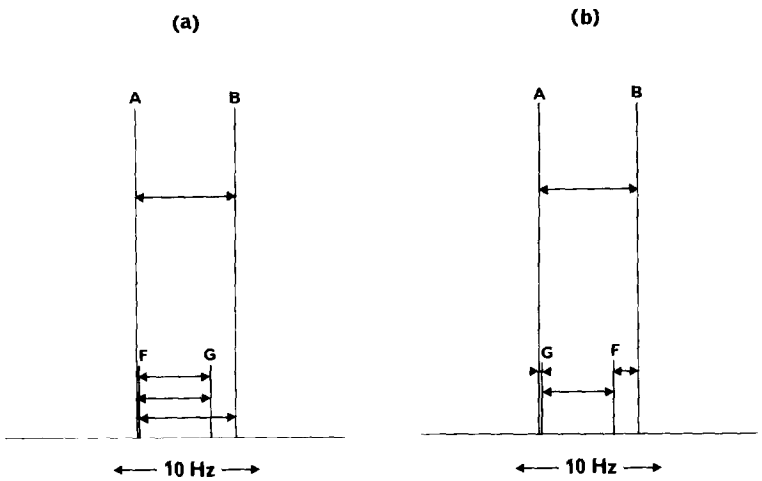

Fig. 5. The two possible assignments of the t-butyl signals arising from the e_0 pair (A,B) and the $s_{1/2}$ pair (F,G). Only case b provided a satisfactory fit with the experimental spectra.

temperature was accounted for in terms of a mixture comprising 82% e_0 rotamers and 18% $s_{1/2}$ rotamers, with the four chemical shifts ν_A, ν_B, ν_F and ν_G distributed in either of two possible ways (Fig. 5). The greater breadth of the lower frequency component of the doublet can be seen to be attributed to the non-equality of the shifts ν_B and ν_F *or* ν_G. The t-butyl spectrum at $-30\,^\circ$C was simulated for both cases (a and b) in Fig. 5 using the rate constant derived from the ^{13}C spectrum at this temperature, and assuming that this single magnitude of rate constant applied equally to the $e_0 \rightleftharpoons e_0$, $e_0 \rightleftharpoons s_{1/2}$ and $s_{1/2} \rightleftharpoons s_{1/2}$ exchanges. Case b gave an excellent fit with the experimental spectrum (Fig. 4) whereas case a was less satisfactory. The spectra for the other temperatures were fitted similarly using the rate constants from the ^{13}C spectra and with the relative rotamer populations held virtually constant but allowing for slight changes of the four chemical shifts. These temperature dependences of the shifts resulted in $\nu_A \approx \nu_G$ and $\nu_B \approx \nu_F$ at the lowest temperature, thus producing a symmetrical 1 : 1 doublet signal.

This analysis provides convincing evidence for the presence of both e_0 and $s_{1/2}$ rotameric forms in low temperature solutions of 1,1′,3,3′-tetra(t-butyl)ferrocene, and also illustrates the sensitivity of ^{1}H dynamic NMR bandshapes to minor species particularly around the coalescence region. It was clearly not possible to distinguish between the three theoretically different rate constants for this dynamic system, but in practice they are likely to differ only by small factors arising from different rotamer population ratios.

1,1′,3,3′-Tetra(phenyl)ferrocene

A variable temperature ^{1}H NMR study was also carried out on the above complex. This was prompted by some earlier studies by Castellani et al. on *sym*-octa(phenyl)ferrocene [11]. These workers had assumed that the heavily substituted Cp rings were rotating rapidly at room temperature. On cooling a THF-d_8 solution of the complex down to $-95\,^\circ$C, spectral changes occurred below ca. $-60\,^\circ$C, but these were explained in terms of slowed and eventually 'frozen' phenyl ring rotation with two phenyls coplanar to the Cp rings and the other two perpendicular to the ring. The spectral changes clearly support this explanation, but the authors also state that there was no evidence of restricted rotation of the two heavily substituted Cp rings even at $-95\,^\circ$C, which seems somewhat improbable. If, however, the complex exists in solution solely as the 180° staggered rotamer (angle defined with respect to the positioning of the two ring C–H bonds), as is found in the solid state, then the NMR spectra will be totally insensitive to *any* rate of Cp rotation! This compound is therefore unsuited to an investigation of the magnitude of rotational restriction of phenyl substituted Cp rings.

It was therefore thought worthwhile to examine the 1,1′,3,3′-tetra(phenyl)ferrocene compound since now any restricted Cp rotation would be clearly visible as a result of interconversion of the ground state e_0 pair of rotamers. Proton spectra from ambient temperature down to ca. $-100\,^\circ$C were therefore recorded but no significant spectral changes were observed, suggesting the absence of any appreciable barriers to rotation of both the phenyl substituted Cp rings and the phenyl groups themselves.

^{13}C CP-MAS spectrum of 1,1′,3,3′-tetra(t-pentyl)ferrocene

In view of the dearth of X-ray data on the present complexes it was thought that

Table 4
^{13}C CP-MAS NMR spectrum of 1,1′,3,3′-tetra(t-pentyl)ferrocene at −120 °C

Group	Carbon Type	Shift(δ [a]/ppm)
Cp	$\geq C-$	97.96, 93.97
	$\geq C-H$	68.32, 65.61 [b]
t-pentyl	$-CH_2$	40.33 [b]
	$\geq C-CH_3$	34.01 [b]
	$\geq C-$	25.08, 23.89
	$-CH_2CH_3$	10.70 [b]

[a] Rel. to Me_4Si. [b] Broader bands due to partially resolved pairs of signals.

solid state NMR spectra might provide alternative structural information. In particular, evidence of any internal molecular movements (viz. ring or substituent rotations) in the solid state was sought. ^{13}C CP-MAS spectra of complex **2** were obtained in the temperature range ambient to −120 °C. The limiting low temperature spectrum consisted of 9 discrete signals, 4 of which were somewhat broader and analysed as partially overlapping pairs. The total spectrum is fully compatible with an e_0 pair of rotamers and the assignments are given in Table 4. These were aided by also recording an NQS spectrum [15] of the solid complex at ambient temperature. On raising the temperature from −120 °C, the only signals to change were those in the region δ 24–34 associated solely with the t-pentyl carbons. At ambient temperature (22 °C) a complex absorption consisting of at least four signals in the range δ 24.7 − 30.0 was detected. This is tentatively interpreted as evidence of contribution from various rotational conformers of the t-pentyl group, but a more rigorous interpretation is not possible. The solid state spectrum was thus compatible with the two substituted Cp rings locked in the eclipsed e_0 rotameric configuration but with the t-pentyl groups undergoing some type of restricted rotation at temperatures above −120 °C.

Previous X-ray crystal data for 1,1′,3,3′-tetra(trimethylsilyl)ferrocene [6] and 1,1′,3,3′-tetra(t-butyl)ferrocene [20] indicate structures with near-eclipsed cyclopentadienyl rings and with the substituents in fully staggered orientations. The present solution and solid-state NMR studies on the t-butyl and t-pentyl analogues are fully compatible with such structures but cannot differentiate between other structures of C_2 or near C_2 symmetry.

Energy barriers of substituted cyclopentadienyl ring rotations

The results of the NMR bandshape analyses of the complexes **1**–**4** are given in Table 5. No data are available for complex **5** as rotation of the diphenyl substituted Cp rings was fast on the NMR chemical shift time scale at all accessible temperatures. The energy barriers are most usefully discussed in terms of the activation parameter $\Delta G^{\ddagger}$ (298 K) where two trends are very apparent.

Firstly, the rotation barriers are in the range 40–57 kJ mol^{-1}, but are 11–16 kJ mol^{-1} lower for ruthenocenes compared to corresponding ferrocenes. This clearly reflects the smaller interannular repulsions of substituents in the ruthenocenes where the inter-ring distance is significantly longer. The relationship between

Table 5

Arrhenius and Eyring activation parameters for ring rotation in 1,1′,3,3′-tetrasubstituted metallocenes.

Metal	Substituent	E_a (kJ mol^{-1})	$\log_{10}(A/s^{-1})$	$\Delta H^{\ddagger}$ (kJ mol^{-1})	$\Delta S^{\ddagger}$ (J K^{-1} mol^{-1})	$\Delta G^{\ddagger}$(298 K) (kJ mol^{-1})
Fe	t-butyl	63.9±0.3	14.3±0.1	61.7±0.3	20.4±1.2	55.6±0.1
Fe	t-pentyl	84.0±1.2	17.6±0.2	81.7±1.2	84.0±4.3	56.7±0.1
Ru	t-butyl	55.6±0.4	15.6±0.1	53.8±0.4	47.5±1.9	39.7±0.2
Ru	t-pentyl	48.5±0.7	13.3±0.2	46.6±0.7	3.1±3.0	45.7±0.2

metallocene inter-ring distance and the rotational energy barrier of pairs of di-t-butyl)metallocene rings can be seen more closely by comparing ferrocene, ruthenocene and uranocene. The inter-ring distances of these metallocenes are 332 pm [21,22] 368 pm [23] and 385 pm [24,25] respectively, and the rotational energy barriers for corresponding tetra(t-butyl)metallocenes are 55.6, 39.7 and 34.7 [7] kJ mol^{-1} respectively. These data establish a clear inverse relationship between these two molecular parameters.

Secondly, the Cp ring rotational barriers are substituent dependent such that t-pentyl > t-butyl ≫ phenyl, with this dependence being more pronounced in the ruthenocene series. This trend reflects the relative steric bulks of the substituents, but shape is also important and the two-dimensional planarity of the phenyl rings presents less restriction to rotation of the Cp rings than the three dimensional bulkiness of alkyl substituents. The most favourable mechanism would appear to involve a dynamic gearing of substituent rotations with Cp ring rotations. Such a mechanism would allow planar phenyl rings to move past each other much more readily than alkyl substituents and would explain the rapid ring rotation of 1,1′,3,3′-tetra(phenyl)ferrocene even at 173 K. These comments are in keeping with all the collected data of ring rotation barriers of substituted ferrocenes (Table 6). These energies can be seen in general to increase with the number and steric size of the Cp ring substituents, although there are certain anomalies but these may simply reflect the approximate nature of some of the earlier data.

Table 6

Measurements in solution of activation barriers ($\Delta G^{\ddagger}$) to ring rotation for substituted ferrocenes

Substituents	$\Delta G^{\ddagger}$/kJ mol^{-1}	Ref
n-Bu	8.28 [a,b]	2
-CMe_2Et	8.57 [a,b]	2
1,1′,3,3′-$(SiMe_3)_4$	46.0 [c]	6
1,1′,3,3′,-$(CMe_3)_4$	54.81 [c]	7
	55.6 [d]	This work
1,1′,3,3′-$(CMe_2Et)_4$	56.7 [d]	This work
1,1′,2,2′,4,4′-$(SiMe_3)_6$	46.02 [c]	8
1,1′,2,2′-$(SiMe_3)_4$4,4′-$(CMe_3)_2$	40.6 [c]	9
1,1′,2,2′,3,3′,4,4′-(i-Pr)$_8$	56.8 [c]	10

[a] T_1 measurements. [b] C_5H_5 ring. [c] Coalescence temperature measurement. [d] Bandshape analysis measurement.

Acknowledgement

We thank the Science and Engineering Research Council for use of the solid-state NMR service at the University of Durham.

References

1 B.E. Mann, in G. Wilkinson, F.G.A. Stone and E.W. Abel (Eds.), Comprehensive Organometallic Chemistry, Vol. 3, Pergamon Press, Oxford, 1982, p. 111.
2 B.E. Mann, C.M. Spencer, B.F. Taylor and P. Yavari, J. Chem. Soc., Dalton Trans., (1984) 2027.
3 R.J. Pazur, D.F.R. Gilson, P.D. Harvey and I.S. Butler, Can. J. Chem., 65 (1987) 1940.
4 H. Adams, N.A. Bailey, B.E. Mann, B.F. Taylor, C. White and P. Yavari, J. Chem. Soc., Dalton Trans., (1987) 1947.
5 J. Okuda, J. Organomet. Chem., 356 (1988) C43.
6 J. Okuda and E. Herdtweck, J. Organomet. Chem., 373 (1989) 99.
7 W.D. Luke and A. Streitwieser, Jr., J. Am. Chem. Soc., 103 (1981) 3241.
8 J. Okuda and E. Herdtweck, Chem. Ber., 121 (1988) 1899.
9 J. Okuda, Chem. Ber., 122 (1989) 1075.
10 H. Sitzmann, J. Organomet. Chem., 354 (1988) 203.
11 M.P. Castellani, J.M. Wright, S.J. Geib, A.L. Rheingold, and W.C. Trogler, Organometallics, 5 (1986) 1116.
12 D.F. Shriver, Manipulation of Air-Sensitive Compounds, McGraw-Hill, New York, 1969.
13 D.A. Kleier and G. Binsch, J. Magn. Reson., 3 (1970) 146.
14 D.A. Kleier and G. Binsch, DNMR3 Program 165, Quantum Chemistry Program Exchange, Indiana University, 1970.
15 S.J. Opella and M.H. Frey, J. Am. Chem. Soc., 101 (1979) 5854.
16 T. Leigh, J. Chem. Soc., (1964) 3294.
17 N.L. Drake and J.R. Adams, J. Am. Chem. Soc., 61 (1939) 1326.
18 P. Kovacic and N.O. Brace, Inorg. Synth., 6 (1960) 172.
19 P.L. Pauson, J. Am. Chem. Soc., 76 (1954) 2187.
20 Z.L. Kaluski, A.I. Gusev, A.E. Kalinin, and Y.T. Struchkov, Zh. Strukt. Khim., 13 (1972) 950.
21 J.D. Dunitz, L.E. Orgel and A. Rich, Acta Crystallogr., 9 (1956) 373.
22 P. Seiler and J.D. Dunitz, Acta Crystallogr., B, 35 (1979) 1068.
23 G.L. Hardgrove and D.H. Templeton, Acta Crystallogr., 12 (1959) 28.
24 A. Zalkin and K.N. Raymond, J. Am. Chem. Soc., 91 (1969) 5667.
25 A. Avdeef, K.N. Raymond, K.O. Hodgson and A. Zalkin, Inorg. Chem., 11 (1972) 1083.